Elastic Scattering of Neutrons from Carbon and Oxygen in the Energy Range 3.0 to 4.7 MeV*

D. LISTER† AND A. SAYRES‡
Columbia University, New York, New York
(Received 11 August 1965)

The elastic scattering of neutrons from oxygen and carbon was studied in the neutron bombarding energy range 3.0 to 4.7 MeV. Angular distributions were obtained by the method of recoiling gas atoms in a proportional counter. Data were taken over the entire energy range in approximately 25-keV intervals, and in smaller intervals near certain resonances. Differential cross sections for $C(n,n)C$ were obtained relative to the total n-p cross section. Similarly, $O(n,n)O$ differential cross sections as well as the $O^{16}(n,\alpha)C^{13}$ total cross section were determined relative to the derived $C(n,n)C$ cross sections. A phase-shift search routine was used to find acceptable least-squares fits to a Legendre-polynomial decomposition of the elastic-scattering results. Energy-level parameters were obtained for five states in O^{17} and are given as follows (in the order: resonance energy relative to the O^{17} ground state in MeV, spin and parity, and dimensionless reduced width): 7.24($\frac{3}{2}^+$, 0.15), 7.69($\frac{3}{2}^-$, 0.07), 7.70($\frac{7}{2}^-$, <0.03), 7.83($\frac{1}{2}^-$, 0.04), and 8.07($\frac{3}{2}^-$, 0.02). Level parameters were also determined for two states in C^{13}: 8.27($\frac{3}{2}^+$, 0.45) and 8.87($\frac{1}{2}^-$, 0.03).

I. INTRODUCTION

THE primary object of this work was to study the spectroscopy of O^{17} in the excitation energy range from 7.0–8.6 MeV by means of the $O^{16}(n,n)O^{16}$ reaction. Total neutron cross-section measurements for O^{16} have indicated the presence of broad and narrow overlapping levels in this energy region.[1,2] The usually difficult problem of determining scattering parameters is simplified, as the entrance channel is composed of a neutron (spin $\frac{1}{2}$) and O^{16}(spin 0) so that the channel spin s can have only the value $s=\frac{1}{2}$. For a given partial wave of relative orbital angular momentum l, the total angular momentum J of the $O^{16}+n$ system is limited to the values $J=l\pm\frac{1}{2}$ and the parity is given by $(-1)^l$. Successful analysis of the differential cross sections in terms of the elastic-scattering phase shifts $\delta(l,J)$ will yield the following level parameters: resonance energy (E_R), spin (J), parity (π), and width (Γ).

In the present investigation $O^{16}(n,n)O^{16}$ differential cross sections were measured over the incident neutron energy range from 3.07–4.73 MeV (excitation energy E_x of O^{17} between 7.0 and 8.6 MeV). Measurements were made in intervals of about 25 keV with an incident neutron energy spread ΔE_n, of about 25 keV over the entire energy range, and in the vicinity of certain resonances in 10-keV intervals with $\Delta E_n \approx 18$ keV.

In the course of this work the $O^{16}(n,\alpha)C^{13}$ total cross section and $C^{12}(n,n)C^{12}$ differential cross section (E_x of C^{13} between 7.78 and 9.32 MeV) were also measured. A phase-shift analysis was performed on the $O^{16}(n,n)O^{16}$ and $C^{12}(n,n)C^{12}$ data and the derived level parameters are presented.

At the time the present work was initiated, previous measurements of the $O^{16}(n,n)O^{16}$ differential cross section in the energy range of this experiment included the work of Baldinger, Huber, and Proctor,[3] Hunzinger and Huber,[4] Sayers,[5] Phillips,[6] and Bostrom, Morgan, Prud'homme, and Sattar.[7] Results of Refs. 4, 6, and 7 appear in a graphical compilation of neutron cross sections.[8] However, only Baldinger *et al.*,[3] extracted phase shifts. They identified three fairly broad levels above $E_x=7.0$ MeV; at $E_n=3.33$ MeV ($E_x=7.28$ MeV, $\frac{3}{2}^+$, $\Gamma=220$ keV), $E_n=3.80$ MeV (7.73 MeV, $\frac{3}{2}^-$, 800 keV), and $E_n=4.40$ MeV (8.29 MeV, $\frac{1}{2}^-$, 280 keV).

Because the various groups of experimenters that have studied the $O^{16}(n,n)O^{16}$ reaction took data in energy steps too coarse to study levels of intermediate width, there was a clear need for a more detailed and systematic study of this reaction.

More recently, Fowler and Johnson[9] have measured $O^{16}(n,n)O^{16}$ differential cross sections at a number of incident neutron energies between 2.25 and 3.90 MeV and extracted phase shifts. Their results were in fair agreement with those of Baldinger *et al.*,[3] regarding the broad $\frac{3}{2}^+$ and $\frac{3}{2}^-$ resonances and also identified two other resonances: $E_n=3.77$ MeV (7.69 MeV, $\frac{5}{2}^-$, 25 keV) and $E_n=3.82$ MeV (7.73 MeV, $\frac{3}{2}^+$, 50 keV).

---

* This work partially supported by the U. S. Atomic Energy Commission.
† Present address: Argonne National Laboratory, Argonne, Illinois.
‡ Present address: Department of Physics, Brooklyn College, New York, New York.

[1] D. J. Hughes and R. B. Schwartz, *Neutron Cross Sections*, Brookhaven National Laboratory Report BNL-325 2nd ed. (Government Printing Office, Washington, D. C., 1958).
[2] J. R. Stehn, M. D. Goldberg, B. A. Magurno, and R. Wiener-Chasman, *Neutron Cross Sections*, Brookhaven National Laboratory Report BNL-325, 2nd ed., Suppl. No. 2 (Office of Technical Services, Department of Commerce, Washington, D. C., 1964), Vol. 1.
[3] E. Baldinger, P. Huber, and W. G. Proctor, Helv. Phys. Acta **25**, 142 (1952).
[4] W. Hunzinger and P. Huber, Helv. Phys. Acta **35**, 351 (1962).
[5] A. Sayres, Bull. Am. Phys. Soc. **6**, 237 (1961).
[6] D. D. Phillips (unpublished). See Ref. 16.
[7] N. A. Bostrom, I. L. Morgan, J. T. Prud'homme, and A. R. Sattar, Wright Air Development Center Report WADC-TR-57-446, 1957 (unpublished).
[8] M. D. Goldberg, V. M. May, and J. R. Stehn, Brookhaven National Laboratory Report BNL-400, 2nd ed. (Office of Technical Services, Department of Commerce, Washington, D. C., 1963), Vol. 1.
[9] J. L. Fowler and C. H. Johnson (private communication).

II. EXPERIMENTAL PROCEDURE

A. Method

The neutron elastic-scattering measurements were made by means of the recoiling atom method,[10] chosen because of the relatively high rate of data accumulation associated with it. The scattering nuclei were present as part of the gas filling of a proportional counter in which the energy of the recoiling nucleus was measured. Application of energy and momentum conservation laws to the elastic scattering process gives the relation,[11]

$$E_r = 4mM/(m+M)^2 E_n \tfrac{1}{2}(1-\cos\theta_{\text{c.m.}}), \qquad (1)$$

where E_r = kinetic energy of the recoiling nucleus, E_n = incident neutron energy, $\theta_{\text{c.m.}}$ = neutron scattering angle in the c.m. system, m = mass of the neutron, and M = mass of the recoil nucleus. From (1) it can be shown that the neutron angular distribution is proportional to the recoil energy distribution. The latter is proportional to the corresponding pulse-height distribution from the detector if W, the average energy loss per electron-ion pair produced in the counter gas, is independent of the recoil energy. This last condition is at least approximately true in practice. For an arbitrary $W=W(E)$ the relationship between the differential cross section, $\sigma(\Omega)$, and the pulse-height distribution, $N(X)$, is given by $\sigma(\Omega) \propto N(X)/W(X)$ where X represents the pulse height corresponding to a given initial recoil energy.

The experimental arrangement is shown in Fig. 1. Neutrons were produced by the reaction $T(p,n)He^3$ ($Q=-0.764$ MeV). Protons from the Columbia University Van de Graaff electrostatic accelerator were incident on a gaseous T_2 target separated from the vacuum of the drift tube by a 0.05-mil thick nickel window. The collimated neutron beam was coaxial with the proportional counter and the proton beam. Recoil spectra were taken in three series of runs, the counter being filled with carbon dioxide (CO_2) in the first series, propane (C_3H_8) in the second, and methane (CH_4) in the third. In each series, data were obtained at the same neutron energies and for the same experimental geometry. Data and backgrounds were determined by recording alternately spectra from the proportional counter with the brass collimator aperture open and then blocked by a brass insert. Background counts due to neutrons produced in the target cell in the absence of tritium gas were negligible. A "long counter,"[12] using a He^3-filled proportional counter as the thermal neutron detector, positioned one meter from the target and 90° to the proton beam, served as a monitor.

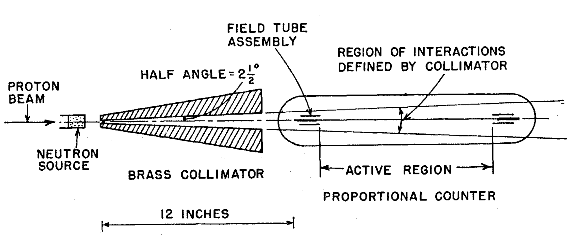

FIG. 1. Experimental arrangement.

In the energy region under investigation the following conditions prevail: (1) Neutron capture by O and C is negligible compared to elastic scattering[1,2]; (2) elastic scattering is the only other open channel in the $C^{12}+n$ interaction, and (3) the $O^{16}(n,\alpha)C^{13}$ ($Q=-2.215$ MeV) cross section is negligible compared to elastic scattering for $E_n<4.1$ MeV.[13] Furthermore, for incident neutron energies greater than 3.1 MeV the group of pulses from the $O^{16}(n,\alpha)C^{13}$ reaction has greater pulse height than pulses due to the most energetic recoils in the CO_2 filling.

B. Apparatus

1. Proportional Counter

Theoretical and practical discussions on proportional counters are well covered in the literature.[11,14] The counter used in this experiment had cylindrical geometry. A 4-mil stainless steel anode wire was positioned axially with respect to a 2.75-in. i.d., 0.125-in. wall stainless steel cylindrical cathode. The $9\frac{7}{8}$-in. long active volume was defined by a pair of $\frac{1}{2}$-in. o.d. field tubes concentric with the center wire, which served to keep the electric field radial over the entire active volume. An important feature of the construction was that all electrical feed-throughs were located off-axis so as not to be in the path of the axially collimated neutron beam.

Commercially available high-purity gases were used for the counter fillings with no further purification. The suppliers listed the following purities: CO_2, 99.9998%; C_3H_8, 99.99 mole%; CH_4, 99.68 mole%. A measure of the resolution was given by noting the shape of the high-energy cutoff of the recoil pulse-height distributions. The resolution was found to be about 3% for proton recoils of 3.07-MeV energy, 10% for 0.87-MeV carbon recoils in both CH_4 and C_3H_8, and 11 and 13%, respectively, for 0.95-MeV carbon ions and 0.74-MeV oxygen ions in CO_2. The average energy expended per electron ion pair in stopping 0.87-MeV carbon ions in CH_4 was observed to be about 30% greater than the same quantity for 3.07-MeV protons, which is in rough agreement with previous observations.[15]

[10] H. H. Barschall and M. H. Kanner, Phys. Rev. **58**, 590 (1940).
[11] S. C. Curran, in *Encyclopedia of Physics*, edited by S. Flügge (Springer-Verlag, Berlin, 1958), Vol. 45, pp. 174 ff.
[12] A. O. Hanson and J. L. McKibben, Phys. Rev. **72**, 673 (1947).
[13] R. B. Walton, J. D. Clement, and F. Boreli, Phys. Rev. **107**, 1065 (1957).
[14] B. B. Rossi and H. H. Staub, *Ionization Chambers and Counters* (McGraw-Hill Book Company, Inc., New York, 1949), Chapt. 4, 7.
[15] A. T. G. Ferguson, in *Fast Neutron Physics*, edited by J. B. Marion and J. L. Fowler (Interscience Publishers Inc., New York, 1960), Part I, p. 179.

2. *Neutron Energy Calibration*

Precautions were taken to determine accurately the neutron energy for reasons to be mentioned below. Proton energies were inferred by the standard procedure of monitoring the field of the 90° momentum-analyzing magnet by means of the nuclear magnetic resonance frequency f of hydrogen calibrated at the $Li^7(p,n)Be^7$ threshold at $E_p = 1.8811$ MeV. The calibration constant k, in the expression,

$$E_p = kf^2(1 - kf^2/2mc^2),$$

where mc^2 = rest energy of the proton, which includes the first-order relativistic correction, was assumed to be constant over the energy range studied. For the analyzing magnet used, past experience has shown that this calculated E_p would be at most greater than the true E_p by about 5 keV at the uppermost energy used.

Tables[16] of neutron energies as a function of proton energy and neutron emission angle for the $T(p,n)He^3$ reaction were used to obtain the average neutron energy E_n after having taken into account proton energy losses in traversing the nickel foil and the tritium, and the variation of neutron energy in the solid angle of the collimated neutron beam. The thickness of the nickel window was ascertained by noting its effect in shifting the $T(p,n)He^3$ threshold energy from the published value[17] of 1.019 MeV. The measured shift was 135±5 keV as compared with a calculated ionization loss of 129 keV for a 0.05-mil nickel thickness.[18] The neutron energies that will be quoted in this paper may be considered accurate to ±10 keV on an absolute scale. Energy differences are accurate to ±5 keV. The mean energy spread of the neutrons was obtained by folding into the energy loss of protons in traversing the tritium a width of 12 keV representing the combined effects of all other energy-spreading factors present. The latter was determined empirically from the observed widths of narrow resonances in $O^{16}(n,\alpha)C^{13}$ when a very thin tritium target was employed.

3. *Electronics*

Pulses from the proportional counter were first fed into a low-noise pre-amplifier, then into a pulse shaper and finally into one-half of a 512-channel pulse-height analyzer. The entire system was linear to ±1%. A running dead-time correction was accomplished by normalizing to the total number of monitor counts that arrived at times when the multichannel analyzer was not "busy."

C. Handling of Data

The reduction of the data was treated in the following manner. Dead-time correction and background subtraction were performed for each run and the results were machine-plotted. Figures 2 and 3 illustrate such results and show pulse-height distributions for CO_2 and C_3H_8, respectively, at $E_n = 3.286$ MeV. The number of proton recoils of energy greater than the upper bias of Fig. 3 were counted in a scaler. The proton recoil con-

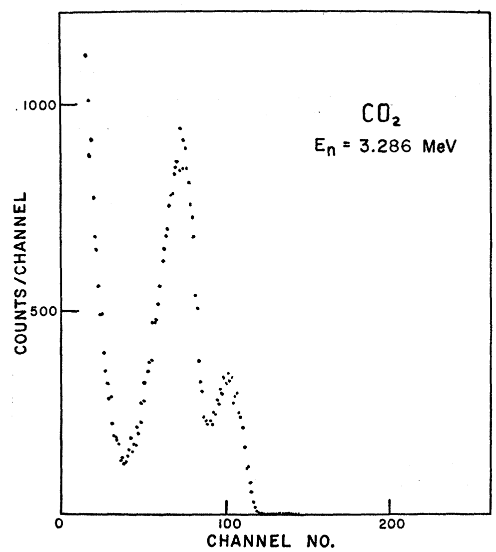

FIG. 2. The pulse-height distribution for the interaction of neutrons with CO_2 observed at 3.286 MeV.

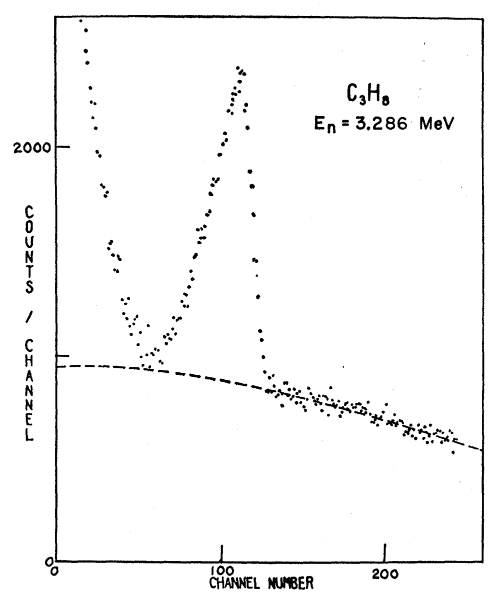

FIG. 3. The pulse-height distribution for the interaction of neutrons with C_3H_8 observed at 3.286 MeV. The higher-energy part has been biased-out electronically. The assumed proton-recoil contribution is shown by the dashed curve.

[16] J. B. Marion and B. Allen, Shell Development Company, Houston, Texas, 1955 (unpublished).

[17] J. E. Brolley, Jr., and J. L. Fowler, in *Fast Neutron Physics*, edited by J. B. Marion and J. L. Fowler (Interscience Publishers Inc., New York, 1960), Part I, p. 73.

[18] J. B. Marion, *1960 Nuclear Data Tables* (U. S. Government Printing Office, Washington, D. C., 1960), Part 3, p. 16.

tribution to the C_3H_8 data was subtracted leaving the pulse-height distribution of the carbon recoils. In Fig. 3, the proton recoil contribution is shown as the dashed curve. Its shape is not quite flat because of wall effect. The $C^{12}(n,n)C^{12}$ scattering is backward-peaked at this energy and its endpoint appears near channel 120. The portion of the dashed curve in the region of the carbon recoils was estimated in a consistent manner on all the C_3H_8 plots so as to join smoothly with the higher channel distribution and take wall and end effects into account. The CH_4 recoil distributions were similarly treated. A check on this procedure was to compare the resulting carbon-recoil distributions with the best published[19,20] $C^{12}(n,n)C^{12}$ angular distributions at energies where they were available. Figure 4(a) shows the resulting carbon recoil distribution at $E_n=3.286$ MeV.

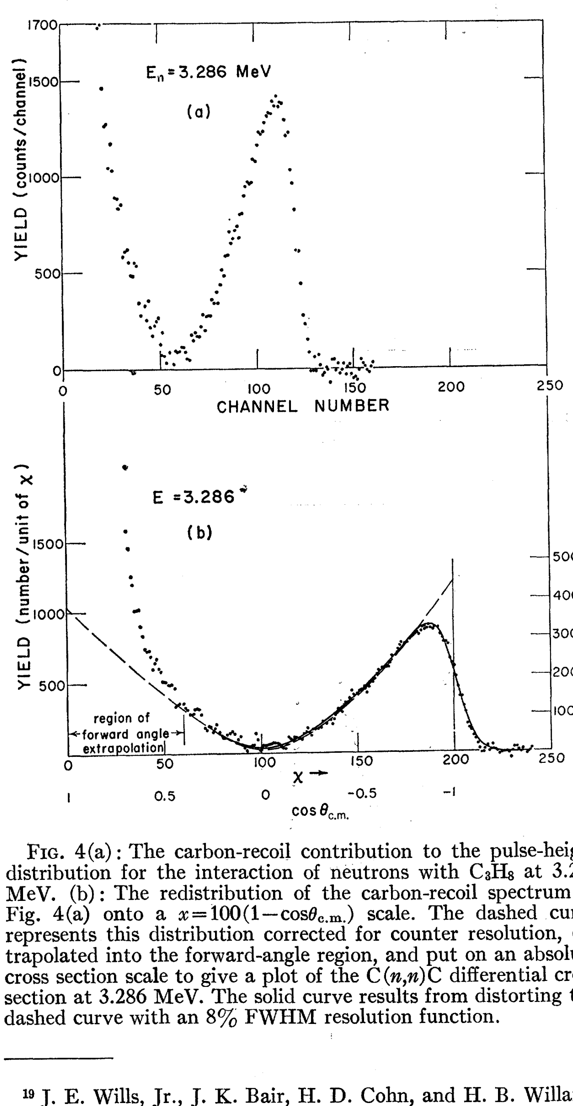

FIG. 4(a): The carbon-recoil contribution to the pulse-height distribution for the interaction of neutrons with C_3H_8 at 3.286 MeV. (b): The redistribution of the carbon-recoil spectrum of Fig. 4(a) onto a $x=100(1-\cos\theta_{c.m.})$ scale. The dashed curve represents this distribution corrected for counter resolution, extrapolated into the forward-angle region, and put on an absolute cross section scale to give a plot of the $C(n,n)C$ differential cross section at 3.286 MeV. The solid curve results from distorting the dashed curve with an 8% FWHM resolution function.

Next, the carbon recoil distribution was converted to an angular distribution, the energy dependence of $\langle W\rangle$ being taken into account. $\langle W\rangle$ was taken to be $\langle W(E)\rangle = W(E_0)+(E-E_0)d\langle W\rangle/dE$. E_0 was some reference energy. Values of $d\langle W\rangle/dE$ for the various recoil ions were obtained from plots of recoil distribution endpoints versus neutron energy. The absolute scale for the differential cross section was obtained by normalizing the estimated number of $p+n$ collisions that occurred within the sensitive volume of the counter to the known $n-p$ total cross section.[21] Also, the angular distributions were corrected for the finite resolution of the counter. This was especially important near the end point of the recoil distribution (i.e., near $\theta=180°$). The large errors in the forward-angle data due to uncompensated low-energy background were avoided by extrapolating the angular distribution curve in this region so that the integrated cross section was equal to the $C^{12}+n$ total cross-section results of Fossan *et al.*,[22] and Bockelman *et al.*[23] Figure 4(b) illustrates these steps for $C^{12}(n,n)C^{12}$ at $E_n=3.286$ MeV.

Extraction of the $O^{16}(n,n)O^{16}$ angular distributions from the CO_2 recoil data was treated in a somewhat similar way. First, the CO_2 recoil pulse-height distribution was redistributed so that the carbon-recoil part was on a $\cos\theta$ scale. Normalization was made by matching the spectrum of carbon recoils of greater energy than the oxygen recoil endpoint to the corresponding part of the previously determined $\sigma(\Omega)[C^{12}(n,n)C^{12}]$ curve, taking into account the distortion due to the finite counter resolution. The oxygen recoil distribution, which remained after the carbon recoil contribution was subtracted from the CO_2 recoil spectrum, was then converted to a differential cross-section curve. The $O^{16}(n,\alpha)C^{13}$ total cross section was obtained from the integrated number of pulses larger than those due to the highest energy carbon recoils. Correction to the (Ω) results was made for counter resolution. A forward angle extrapolation was performed such that $\int\sigma(\Omega)[O^{16}(n,n)O^{16}]d\Omega=$ the total elastic-scattering cross section. The latter was taken to be the Wisconsin total neutron cross-section results[22,23] minus $\sigma_\alpha[O^{16}(n,\alpha)C^{13}]$. It was necessary to increase the energy scale of the work of Fossan *et al.*,[22] by 10 keV to conform with the energies we found for the narrow states in the vicinity of E_n between 4.5 and 4.7 MeV. Figures 5(a) and (b) illustrate the procedure for extracting $\sigma(\Omega)[O^{16}(n,n)O^{16}]$ at $E_n=3.286$ MeV.

The $O^{16}(n,n)O^{16}$ and $C^{12}(n,n)C^{12}$ differential cross-section curves were Fourier analyzed as a sum of

[19] J. E. Wills, Jr., J. K. Bair, H. D. Cohn, and H. B. Willard, Phys. Rev. **109**, 891 (1958).

[20] R. W. Meier, P. Scherrer, and G. Trumpy, Helv. Phys. Acta **27**, 577 (1954).

[21] J. L. Gammel, in *Fast Neutron Physics*, edited by J. B. Marion and J. L. Fowler (Interscience Publishers Inc., New York, 1963), Part II, p. 2185.

[22] D. B. Fossan, R. L. Walter, W. E. Wilson, and H. H. Barschall, Phys. Rev. **123**, 209 (1961).

[23] C. K. Bockelman, D. W. Miller, R. K. Adair, and H. H. Barschall, Phys. Rev. **84**, 69 (1951).

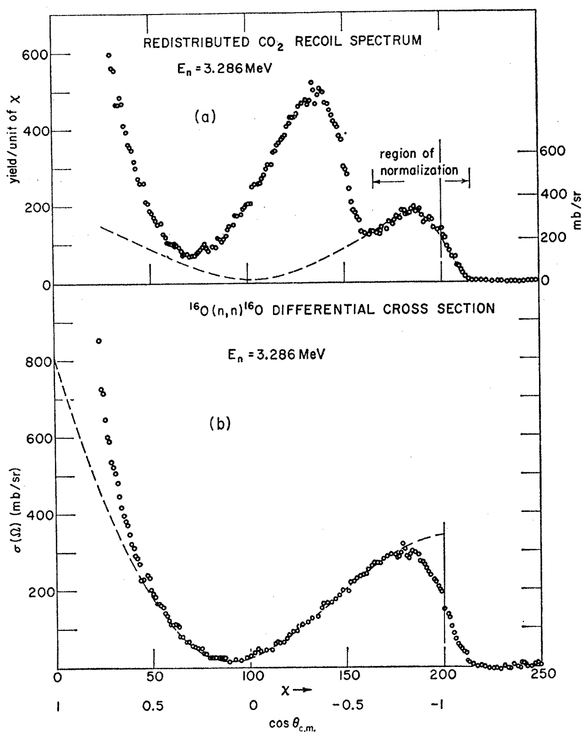

FIG. 5(a): The redistributed spectrum for the interaction of neutrons with CO_2 at 3.286 MeV. The carbon-recoil part is on a $x=100(1-\cos\theta_{c.m.})$ scale. The dashed curve represents the result of distorting the ideal $C(n,n)C$ angular distribution with a 10% FWHM resolution function. (b): The $O^{16}(n,n)O^{16}$ angular distribution on an absolute cross-section scale before (points) and after (dashed curve) forward-angle extrapolation and correction for resolution.

Legendre polynomials through the sixth order:

$$\sigma(\Omega)=\sum_{L=0}^{6} A_L P_L(\cos\theta_{c.m.}). \qquad (2)$$

We used Price's method[24] to obtain the expansion coefficients. This Fourier analysis served a double purpose. First, it is a concise form in which to express the angular distributions. Second, it is a useful intermediate step in carrying out the phase-shift analysis (see Sec. V). The cutoff of the series (2) at $L=6$ was necessitated by the effective experimental angular resolution. It corresponded to ignoring contributions from partial waves of $l\geq 4$, which was justifiable on physical grounds since neutron penetrabilities for $l\geq 4$ waves are quite small at these energies

III. ERRORS

The various steps in the procedure for reduction of data described in Sec. II introduced a variety of interacting systematic uncertainties. The net effects of all the uncertainties fell into three main categories: Statistical errors, normalization errors, and all others. How these uncertainties are taken into account in the phase-shift analysis is discussed in Sec. V.

A. Statistical Errors

Statistical errors contributed an average uncertainty over back angles of from 5 to 9 mb/sr in the $O^{16}(n,n)O^{16}$ differential cross section and from 8 to 13 mb/sr in the $C^{12}(n,n)C^{12}$ differential cross section.

As applied to the present analysis, Price's method could not yield quantitatively the uncertainties in the Legendre polynomial expansion coefficients arising from statistical fluctuations in the pulse-height distributions. A fair indication of these errors was, however, found by performing a least-squares fit to the data in the region $0.4<\cos\theta<-0.8$, with each channel given unit weight and with the total cross section value (i.e., A_0) held fixed. Then the statistical uncertainty in a coefficient, defined as the deviation in that coefficient alone needed to double the value of χ^2 with respect to its minimum value, was calculated. The errors obtained are shown in Table I.

B. Normalization Errors

Normalization errors were of two kinds. The first group included those that directly affected $\sigma(\Omega)$ at back angles but left the total elastic-scattering cross section σ_n(elastic) unchanged. Examples are the normalization of $\sigma(\Omega)[C^{12}(n,n)C^{12}]$ to $\sigma_T(n\text{-}p)$ through the integrated proton-recoil counts in the C_3H_8 runs, and the normalization of $\sigma(\Omega)[O^{16}(n,n)O^{16}]$ to the back-angle $C+n$ scattering. As a result of this kind of uncertainty, $\sigma(\Omega)$ would be in error at back angles by a constant fraction; and the computed $\sigma(\Omega)$ at forward angles would be in error in the opposite direction in a more complicated way. It turned out that the errors in the A coefficients could be related to all the A coefficients through a linear matrix with a multiplicative constant, ϵ, denoting the size of the error. For $C+n$ scattering $|\epsilon|$ was about 8% and for $O+n$ scattering $|\epsilon|$ was about 17%.

The second kind of normalization error is associated with uncertainties in the normalization to σ_n (elastic) values and affects only the computed $\sigma(\Omega)$ at forward angles. Again uncertainties were propagated into the A coefficients in a way that could be expressed as a linear matrix with a multiplicative constant, ϵ. In the case of $C^{12}(n,n)C^{12}$, $|\epsilon|\sim 3\%$ (the quoted statistical error in the published total neutron cross section,[22]

TABLE I. Statistical errors in A coefficients.

Reaction	Range of error ($\pm$) in mb/sr A_0	A_1	A_2	A_3	A_4	A_5	A_6
$O^{16}(n,n)O^{16}$	5–9	13–22	14–23	17–28	18–31	19–32	23–39
$C^{12}(n,n)C^{12}$	8–13	20–32	23–35	28–42	30–45	32–48	37–58

[24] P. C. Price, Phil. Mag. 45, 237 (1954).

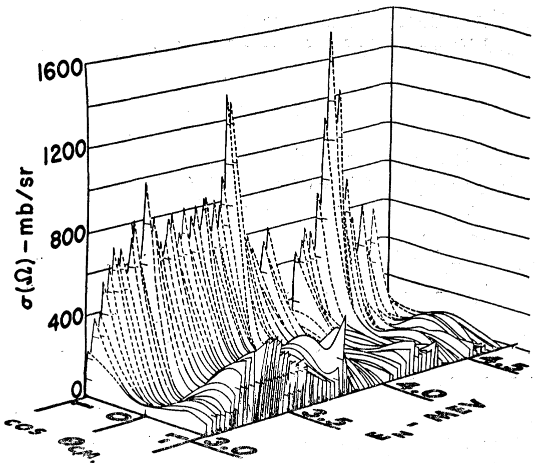

FIG. 6. $O^{16}(n,n)O^{16}$ differential cross sections as a function of c.m. scattering angle and neutron energy.

except for E_n between 4.20 and 4.25 MeV, where $|\epsilon|\sim 6\%$. In the $O+n$ scattering case the situation was somewhat more complex owing to the existence of several important relatively narrow resonances and the presence of the $O^{16}(n,\alpha)C^{13}$ reaction channel. Here

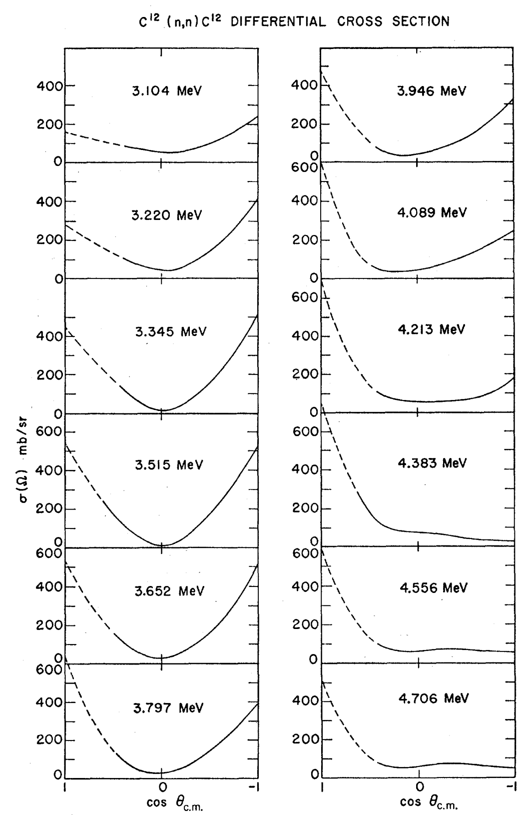

FIG. 7. Typical differential cross-section curves for $C^{12}(n,n)C^{12}$ at various energies over the energy range studied. Correction for counter resolution has been included. The dashed line portions represent the forward-angle extrapolations.

we can write $|\epsilon|=|\epsilon(\sigma_n, \text{ statistical})|+|\epsilon(\text{reaction})|+|\Delta\sigma_n(10 \text{ keV})/\sigma_T|$, where the first and second terms are self-explanatory. The third term represents the effect of an assumed 10-keV uncertainty in our energy calibration relative to that of the total neutron cross-section work.[22,23] These terms had roughly the following values: $|\epsilon(\sigma_n, \text{ statistical})|\sim 3\%$; $|\epsilon(\text{reaction})|\simeq 0.17\sigma_\alpha \times[O^{16}(n,\alpha)C^{13}]/\sigma_T\sim 3\%$ maximum, but was usually negligible; and $|\Delta\sigma_n(10 \text{ keV})/\sigma_T|$ which could be as high as 30% on the steep slopes of certain resonances, but usually was <10%. Because of the forward-angle extrapolation procedure, practically no forward-angle errors in the $C^{12}(n,n)C^{12}$ results propagated into the $O^{16}(n,n)O^{16}$ results.

C. Miscellaneous Errors

Sources of various other uncertainties together with their maximum contributions appear in Table II.

IV. CROSS-SECTION RESULTS

The $\sigma(\Omega)[O^{16}(n,n)O^{16}]$ results are displayed in Fig. 6 as a function of energy and the derived Fourier coefficients, A_L, of Eq. (2) are listed in Table III.

Table IV lists the A coefficients for $\sigma(\Omega)[C^{12}(n,n)C^{12}]$. In Fig. 7 are shown $\sigma(\Omega)[C^{12}(n,n)C^{12}]$ results at a number of energies to illustrate how the angular distributions vary over the range of energies studied. The solid-line portions of the curves in Figs. 6 and 7 represent visually drawn curves through the data and include correction for counter resolution, while the dashed-line portions represent the forward-angle extrapolations.

The measured $O^{16}(n,\alpha)C^{13}$ total cross sections are plotted as the circles and crosses of Fig. 8 and have not been corrected for wall or end effects. Such a correction would be no more than 4%, and is small compared

TABLE II. Miscellaneous sources of error.

Sources of uncertainties	Maximum expected contribution
1. Impurities	1%
2. Multiple scattering	1%
3. Pile up of pulses	1%
4. Wall and end effects	1%
5. Proton-recoil extrapolation	Mainly, ~20 mb/sr in the coefficient A_1 in $C+n$ scattering. Also, a carry-over of ~4 mb/sr in A_2 in $O+n$ scattering.
6. Finite resolution of counter	Negligible for A_0, increasing with the order of A coefficient to about 20% for A_6.
7. Energy spread of neutron beam	Averaged each A coefficient over the energy spread.
8. Quadratic approximation for forward-angle extrapolation	Individual uncertainties in any A coefficient depended in part on values of the other A coefficients. The effect was negligible for the low-order coefficients, but could be appreciable for high-order coefficients.

TABLE III. A Coefficients for neutron elastic scattering from oxygen.

E (MeV)	A_L (mb/sr) A_0	A_1	A_2	A_3	A_4	A_5	A_6
	Energy spread of neutron beam = 25 keV						
3.066	115	54	66	21	−34	−1	7
3.104	126	83	119	71	−16	−6	7
3.127	135	76	137	77	−28	−3	14
3.150	147	110	196	114	−15	−6	11
3.167	155	110	222	132	−24	2	17
3.196	171	126	268	148	−16	−1	2
3.220	187	102	260	143	−43	−14	18
3.245	201	79	319	140	−41	3	13
3.266	214	76	339	130	−38	−12	11
3.286	224	92	370	136	−26	−4	9
3.306	232	100	380	126	−34	−14	4
3.349	241	105	376	94	−9	−12	4
3.372	240	102	342	81	−12	−7	14
3.396	239	91	309	48	−7	−4	6
3.420	241	113	299	46	−7	−10	11
3.442	249	154	309	81	1	−7	−6
3.464	243	162	297	81	26	−1	−14
3.488	234	154	256	45	2	−11	4
3.513	233	171	247	50	5	−3	−6
3.521	232	197	278	94	17	−12	−6
3.542	236	178	246	49	−6	−28	−5
3.563	237	203	245	77	12	−9	−4
3.585	236	221	253	106	12	−16	−5
3.608	239	231	246	114	28	−18	−15
3.630	238	236	244	128	22	−19	−11
3.654	237	213	197	107	−4	−24	−9
3.675	233	230	214	144	21	−26	1
3.702	224	197	166	134	18	−32	−9
3.724	232	207	183	177	41	−45	9
3.749	239	219	231	216	93	−72	−6
3.773	303	179	419	322	198	−53	5
3.799	286	226	417	297	41	78	−47
3.823	202	170	184	131	−32	39	−11
3.847	196	200	180	161	5	13	−10
3.874	190	189	146	143	4	10	−7
3.898	182	183	125	114	−7	−0	10
3.925	177	149	76	73	−24	−14	5
3.950	170	175	105	93	−2	−9	−8
3.972	167	185	120	90	−5	−8	−8
3.995	166	194	111	69	−14	−6	−0
4.020	153	211	161	103	2	−8	−14
4.047	121	136	122	56	−2	−12	−7
4.067	104	113	122	93	25	−2	−17
4.090	88	40	61	49	−1	−7	−2
4.117	83	−1	14	17	−13	−9	5
4.141	85	−0	33	15	−39	14	−8
4.166	104	10	86	−9	−35	−8	10
4.188	150	86	186	47	−17	−6	−1
4.212	154	104	175	76	3	−2	−9
4.237	140	125	161	101	44	5	−24
4.263	113	59	78	30	17	−1	−15
4.288	105	116	160	93	68	7	−13
4.311	141	176	232	110	80	6	−30
4.337	219	312	341	179	60	1	−25
4.361	223	396	449	357	136	−0	−30
4.383	181	317	353	305	101	−10	−29
4.409	171	208	202	204	28	−28	−3
4.435	149	185	187	194	48	−27	−31
4.458	135	194	201	195	59	−19	−22
4.482	96	126	126	124	23	−19	−4
4.507	99	126	138	153	56	−10	−18
4.531	99	43	64	68	0	−13	−11
4.557	131	113	132	163	86	−23	−33
4.585	97	39	−3	78	42	−22	−21
4.609	116	87	66	118	72	−27	−22
4.634	89	−1	−39	63	11	−28	7
4.658	110	124	123	160	64	−11	−15
4.682	84	36	−5	45	14	−17	−11
4.705	79	47	11	58	27	−11	−5
4.730	75	28	−14	33	16	−11	−9

E (MeV)	A_L (mb/sr) A_0	A_1	A_2	A_3	A_4	A_5	A_6
	Energy spread of neutron beam = 18 keV						
3.245	200	76	303	140	−54	−1	2
3.256	210	74	327	155	−55	−4	19
3.267	216	103	347	156	−46	−4	10
3.274	218	110	358	162	−45	−5	7
3.278	220	78	343	130	−58	−3	21
3.282	223	68	330	114	−67	−5	8
3.296	229	78	330	121	−58	−4	6
3.301	233	110	368	146	−41	−10	4
3.312	236	95	378	136	−29	−15	6
3.415	242	140	311	64	−3	−17	−0
3.421	238	130	298	43	−16	−19	4
3.433	242	177	335	84	23	−15	−15
3.443	252	164	331	78	17	−18	−11
3.451	259	179	313	84	35	−23	−23
3.463	244	211	312	106	39	−16	−18
3.473	240	187	298	76	12	−14	−15
3.484	237	181	268	59	1	−5	4
3.486	236	197	305	102	24	−9	−13
3.495	238	189	276	74	10	−14	−21
3.503	236	181	270	66	9	−14	−19
3.505	236	178	268	56	11	−13	−8
3.513	235	171	253	47	3	−6	1
3.521	237	176	240	36	−22	−28	−9
3.647	240	233	219	106	0	−34	−20
3.656	241	222	225	122	29	−33	−2
3.664	239	209	187	106	16	−35	−2
3.674	239	206	201	126	11	−29	−12
3.684	237	221	222	155	30	−40	−6
3.696	236	251	231	168	38	−44	−13
3.705	237	247	232	165	23	−39	4
3.715	235	234	228	179	45	−46	−7
3.734	236	198	183	158	35	−56	−5
3.745	239	244	250	221	74	−64	2
3.757	255	229	263	250	99	−83	−2
3.767	284	277	383	329	171	−93	−11
3.777	331	231	517	362	206	−83	−10
3.786	353	275	612	395	166	−13	−60
3.797	319	262	515	312	68	45	−44
3.807	245	169	289	156	−29	58	−50
3.816	211	170	229	132	−32	39	−27
3.825	204	188	200	131	−33	19	−25
4.498	99	136	147	150	50	−15	−19
4.513	101	114	122	138	31	−15	−12
4.521	102	66	78	94	13	−19	−5
4.531	105	87	115	124	32	−12	−8
4.540	117	81	139	131	43	−9	−14
4.549	131	87	121	135	42	−11	−39
4.558	127	105	124	152	69	−32	−22
4.569	106	85	67	133	72	−22	−34
4.583	99	59	23	107	59	−20	−33
4.592	98	74	37	115	53	−24	−20
4.602	104	84	51	112	58	−17	−31
4.613	107	80	58	110	64	−29	−33
4.622	102	41	30	89	39	−38	−6
4.633	100	56	35	96	19	−30	−3
4.644	100	66	39	104	22	−34	1
4.655	104	108	104	154	65	−15	−29
4.665	96	104	106	139	60	−4	−14

TABLE IV. A Coefficients for neutron elastic scattering from carbon.

E (MeV)	A_0	A_1	A_2	A_3	A_4	A_5	A_6
				A_L (mb/sr)			
	Energy spread of neutron beam = 25 keV						
3.068	92	−42	46	−14	−1	3	−1
3.104	109	−26	95	−18	−13	4	7
3.128	118	−56	106	−23	−14	9	5
3.149	118	−46	134	−21	−19	4	11
3.169	142	−48	192	−29	−32	20	3
3.194	140	−24	187	−21	−30	7	17
3.220	150	−36	210	−33	−24	4	16
3.243	156	−8	245	−11	−25	2	17
3.266	164	−29	246	−31	−38	4	25
3.286	169	−14	268	−31	−49	7	20
3.307	175	−15	283	−25	−42	8	18
3.327	182	5	309	−8	−32	4	15
3.346	186	−6	314	−29	−34	10	13
3.373	188	−14	306	−30	−45	4	24
3.395	198	3	347	7	−22	3	18
3.419	198	−3	335	−1	−33	2	9
3.439	195	−19	323	−15	−41	6	25
3.465	198	−1	328	−14	−45	−3	26
3.492	197	23	348	0	−42	−2	13
3.515	201	9	354	1	−29	1	21
3.518	198	6	334	−16	−35	−1	23
3.540	191	−14	312	−32	−40	3	28
3.562	199	7	333	−10	−31	−4	24
3.584	199	14	335	1	−25	−5	22
3.606	198	37	351	23	−18	−6	12
3.629	199	34	351	24	−1	−4	6
3.652	196	4	329	2	−9	−3	18
3.675	195	43	343	23	−10	−4	15
3.700	195	63	374	67	10	−9	7
3.723	189	41	324	30	3	−8	16
3.748	190	54	331	43	4	−9	11
3.772	183	41	289	35	−7	−9	12
3.797	185	62	319	69	13	−7	1
3.821	178	30	276	42	1	−13	0
3.847	173	47	288	68	5	−3	−4
3.872	168	57	283	62	5	−11	−2
3.897	160	42	263	59	13	−7	−10
3.922	157	25	237	54	2	−6	−1
3.946	156	33	245	53	16	−10	−11
3.970	153	54	258	72	30	−6	−7
3.996	153	−6	200	32	14	−11	−6
4.021	148	45	218	75	28	−10	−24
4.044	149	45	233	79	33	−6	−16
4.070	149	86	262	124	46	−2	−18
4.089	164	57	226	185	26	−56	57
4.115	145	60	223	109	40	−2	−13
4.139	147	53	200	82	34	−9	−16
4.166	148	94	235	114	54	1	−15
4.188	144	101	214	93	46	−8	−13
4.214	154	165	240	101	60	−9	−17
4.236	166	242	303	164	97	−10	−29
4.262	169	225	208	103	56	−11	−6
4.287	166	247	196	96	51	−21	−10
4.310	165	258	204	110	47	−15	−0
4.336	160	253	198	111	46	−4	−7
4.359	155	272	238	143	49	−8	−13
4.384	153	249	205	126	45	−17	−26
4.408	148	217	182	109	35	−10	−18
4.433	146	222	198	123	42	−13	−20
4.456	143	231	232	161	55	−8	−9
4.480	138	218	216	145	56	−4	−9
4.506	135	221	236	169	73	−8	−21
4.531	129	184	194	135	48	−12	−15
4.557	128	164	168	115	34	−16	−10
4.582	125	157	167	126	34	−21	−20
4.606	120	148	156	112	36	−21	−11
4.632	120	110	94	76	15	−16	−4
4.657	116	150	156	109	32	−11	−18
4.682	114	145	157	117	41	−14	−19
4.706	114	133	140	113	32	−16	−14
4.729	112	123	132	101	29	−12	−12

with the over-all uncertainty in $\sigma_\alpha[O^{16}(n,\alpha)C^{13}]$ of about 20%.

V. EXTRACTION OF SCATTERING PARAMETERS

A. Phase-Shift Analysis

The elastic-scattering differential cross section for the interaction between a neutron (spin $\frac{1}{2}$) and a spin-0 nucleus for the case of unpolarized neutrons and a spin-insensitive detector is given by[25]

$$\sigma(\Omega)=\frac{1}{2k^2}\Big\{\Big|\sum_{l=0}^{\infty}\big[(l+1)\sin\delta_l^+\exp(i\delta_l^+)+l\sin\delta_l^-\exp(i\delta_l^-)\big]P_l(\cos\theta)\Big|^2+\sin^2\theta\Big|\sum_{l=0}^{\infty}\big[\sin\delta_l^+\exp(i\delta_l^+)-\sin\delta_l^-\exp(i\delta_l^-)\big]P_l'(\cos\theta)\Big|^2\Big\},\quad (3)$$

where $\delta_l^\pm=\delta(l,J=l\pm\frac{1}{2})$ denotes the (l,J) phase shift, $P_l(\cos\theta)=l$th-order Legendre polynomial, $P_l'(\cos\theta)=dP_l(\cos\theta)/d(\cos\theta)$, and k = wave number in the center-of-mass system. If elastic scattering is the only open channel, all the phase shifts are real. If nonelastic channels are also important, the phase shifts are complex quantities, and the problem of determining them becomes considerably more difficult.

Pisent[26] has recently discussed the problems attending phase-shift analysis of angular distributions in elastic scattering. First, there are the "inherent" ambiguities,[27] for which $\sigma(\Omega)$ is unchanged: (a) If the signs of all the phase shifts are simultaneously reversed, and (b) if $\delta(l,l+\frac{1}{2})$ and $\delta(l,l-\frac{1}{2})$ are interchanged for all l simultaneously. In addition, there may be "accidental" ambiguities, i.e., two or more "independent" sets of phase shifts not related by the transformations mentioned above, yet satisfying $\sigma(\Omega)$ within experimental error at a given energy.

The following requirements, however, are usually enough to relieve all the ambiguities. (1) The phase shifts should vary with energy in a "physical" way. That is, (a) they should be continuous functions of energy; (b) there should be no unusual variation of too many phase shifts together to account for resonances; and (c) over a single resonance, one phase shift should increase with increasing energy with a total increase of approximately 180°, the other phase shifts remaining fairly constant. (2) Nonresonant phase shifts should be given approximately by the "potential" scattering phase shifts; i.e., phase shifts calculated for scattering from an appropriate single-particle potential. (3) The phase shifts should join with those obtained at lower energies, if available.

25 C. L. Critchfeld and D. C. Dodder, Phys. Rev. **76**, 602 (1949).
26 G. Pisent, Helv. Phys. Acta **36**, 248 (1963).
27 J. M. Blatt and L. C. Biedenharn, Rev. Mod. Phys. **24**, 258 (1952).

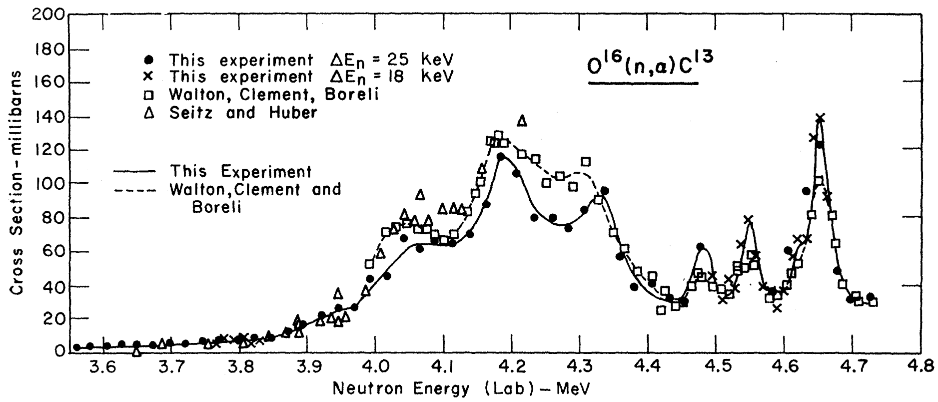

FIG. 8. The $O^{16}(n,\alpha)C^{13}$ total cross section plotted as a function of neutron energy. Comparison with the results of Walton, Clement, and Boreli (Ref. 13) and Seitz and Huber (Ref. 40) is shown.

In principle, if n is the number of phase shifts involved, an n-dimensional search for all independent phase-shift solutions would be desirable at each energy. One would then apply the various criteria of reasonable physical behavior in order to single out the best solution. However, such a complete search program was not practical in this instance because it would have required an excessive amount of computer time.

In the present work, the extraction of phase shifts from the angular distributions was handled in the following way. First, we note that the right-hand side of (3) can be expressed as the sum of Legendre polynomials[27]:

$$\sigma(\Omega)=1/2k^2\sum_L B_L P_L(\cos\theta). \tag{4}$$

In (4), the B coefficients contain the entire dependence of $\sigma(\Omega)$ on the phase shifts, whereas, the k^{-2} and $P_L(\cos\theta)$ factors contain the energy and angular dependences, respectively. Values of the B coefficients up to $L_{\max}=6$ were obtained from the A coefficients of Sec. II and were plotted versus E_n. Smooth curves were drawn visually through the points such that possible resonances

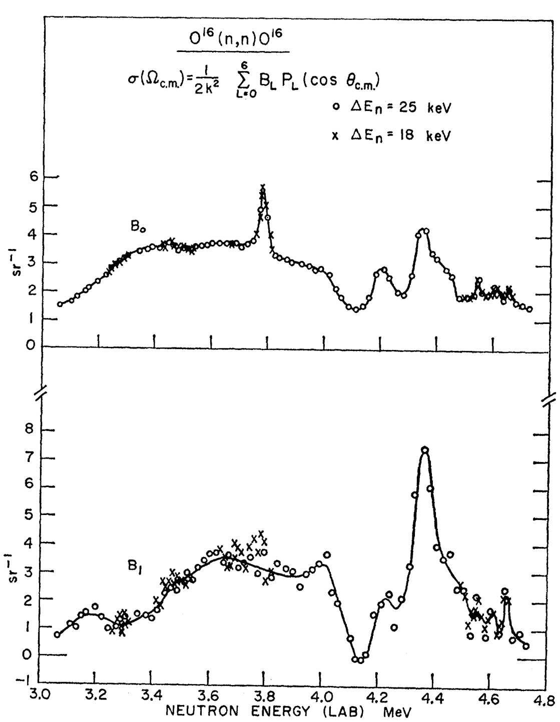

FIG. 9. The coefficients B_0 and B_1 in the expansion

$$\sigma(\Omega)[O^{16}(n,n)O^{16}]=(2k^2)^{-1}\sum_{L=0}^{6} B_L P_L(\cos\theta_{\text{c.m.}})$$

plotted as a function of neutron energy. The solid curves serve to guide the eye and were used for the interpolation of the values of these coefficients in the phase-shift analysis.

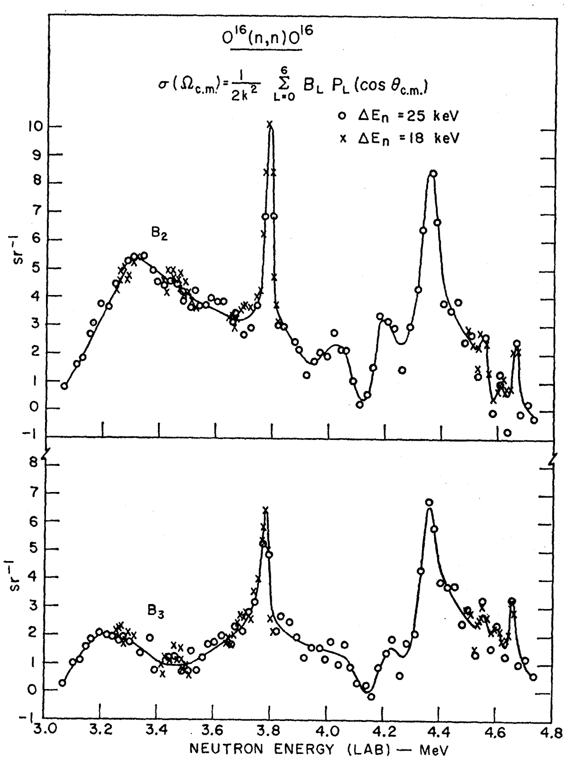

FIG. 10. The coefficients B_2 and B_3 in the expansion

$$\sigma(\Omega)[O^{16}(n,n)O^{16}]=(2k^2)^{-1}\sum_{L=0}^{6} B_L P_L(\cos\theta_{\text{c.m.}})$$

plotted as a function of neutron energy. The solid curves serve to guide the eye and were used for the interpolation of the values of these coefficients in the phase-shift analysis.

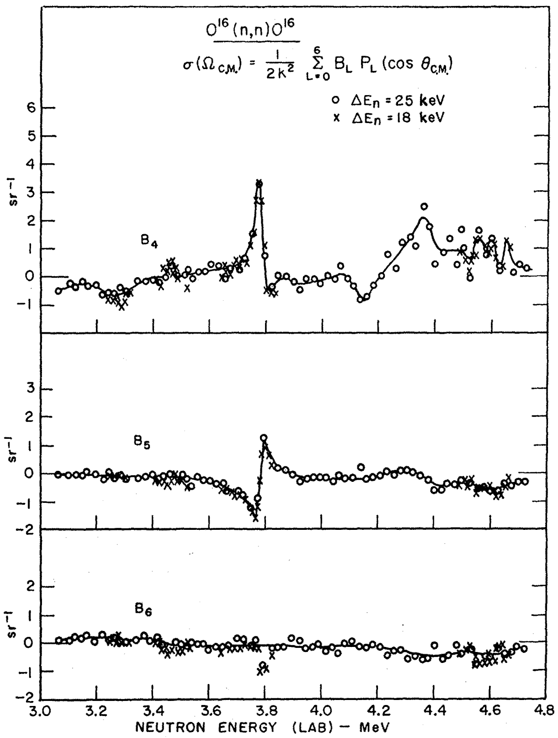

FIG. 11. The coefficients B_4, B_5, and B_6 in the expansion,

$$\sigma(\Omega)[O^{16}(n,n)O^{16}]=(2k^2)^{-1}\sum_{L=0}^{6} B_L P_L(\cos\theta_{\mathrm{c.m.}}),$$

plotted as a function of neutron energy. The solid curves serve to guide the eye and were used for the interpolation of the values of these coefficients in the phase-shift analysis.

of width $\Gamma \ll$ neutron energy spread were ignored. Figures 9–11 and Fig. 12 are plots of the B coefficients for $O^{16}(n,n)O^{16}$ and $C^{12}(n,n)C^{12}$, respectively, with the curves used for them superposed. Next, the B values were read from the curves at a selected energy in a low-energy region where all the B's were varying relatively smoothly with energy. Trial sets of phase shifts were chosen from previously published results in the case[19,20] of $C^{12}(n,n)C^{12}$. For $O^{16}(n,n)O^{16}$ the calculated single-particle potential phase shifts of Kolesov *et al.*,[28] were used. The B coefficients and the trial set of phase shifts were fed into a computer search code that (a) varied singly or in pairs any number of the phase shifts, each over 180° (a full cycle, since the phase shifts enter as $\exp[i2\delta(l,J)]$, (b) calculated for each set of phase shifts, $\delta'(l,J)$, so generated, the quantity χ^2, defined as

$$\chi^2=\sum_{L=0}^{6} 2/2L+1(B_L'-B_L)^2,$$

where $B_L = L$th experimentally determined coefficient and $B_L' = L$th coefficient constructed from the $\delta'(l,J)$; (c) kept the $\delta'(l,J)$ sets that gave the 21 lowest values of χ^2. This last procedure involved a gradient descent method in which all the phase shifts of a set were allowed to vary simultaneously.

The 21 resulting good-fit sets of phase shifts were grouped into "independent" sets and new searches were performed at the same energy starting with these sets to generate, if possible, other independent sets. For example, six independent sets were found for $O^{16}(n,n)O^{16}$ at the first energy selected, $E_n = 3.30$ MeV, and two for $C^{12}(n,n)C^{12}$ at $E_n = 3.10$ MeV. Each resulting independent solution together with the appropriate B coefficient then served as input to similar searches at a second energy chosen reasonably close to the starting energy.

This procedure was repeated over the energy range as far as it could successfully be applied. For $C^{12}(n,n)C^{12}$ this included the entire energy range studied; for $O^{16}(n,n)O^{16}$ it was $3.07 < E_n < 4.20$ MeV. In each case, imposition of the abovementioned requirements of "physical" behavior on the phase shifts narrowed down the number of possible solutions to just one.

Some indication of the uncertainties in the phase shifts was obtained by going back and using the search routine at a given energy, and taking as the initial set of phase shifts their most likely values. $\sigma(\Omega)$ was found in many instances to be much less sensitive to certain simultaneous variations of the phase shifts than to individual variation of the phase shifts about their "best" values.

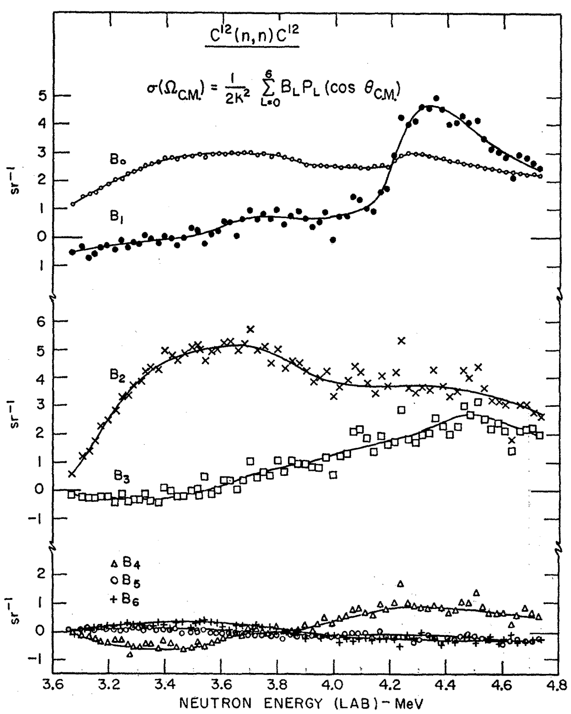

FIG. 12. The B-coefficients in the expansion,

$$\sigma(\Omega)[C^{12}(n,n)C^{12}]=(2k^2)^{-1}\sum_{L=0}^{6} B_L P_L(\cos\theta_{\mathrm{c.m.}})$$

plotted as a function of neutron energy. The solid curves serve to guide the eye and were used for the interpolation of the values of these coefficients in the phase-shift analysis.

[28] V. E. Kolesov, V. P. Korotkikh, and V. G. Malashkina, Izvest. Akad. Nauk, SSSR Ser. Fiz. 27, 903 (1963).

In addition, the 25-keV wide resonance in $O^{16}(n,n)O^{16}$ at $E_n=3.78$ MeV, which was too narrow to be analyzed by the method described above, was studied in the following way. Differential cross sections were artifically generated at ten energies over the resonance for the three cases: each of $\delta(2,\frac{5}{2})$, $\delta(3,\frac{5}{2})$, or $\delta(3,\frac{7}{2})$ alone changing over the resonance according to the dispersion formula,

$$\tan^{-1}\delta(l,J)=\Gamma/2/E_R-E$$

with the other two set equal to zero. It was not necessary to consider $l>3$ as these would result in unreasonably large reduced widths for this level. Interpolated values were used for the remaining phase shifts. The angular distributions so generated were compared with the observed differential cross sections. Figure 13 illustrates this comparison at four of the energies used. Note that no energy averaging was included in the calcluted curves. These comparisons clearly indicated an assignment of $J^\pi=\frac{7}{2}^-$.

The resulting phase shifts for $O^{16}(n,n)O^{16}$ are shown in Fig. 14 and those for $C^{12}(n,n)C^{12}$ in Fig. 15. In these figures, the points represent the best values of the phase shifts at energies where they were determined. The error bars are but a rough indication of uncertainties at selected energies. Smooth curves have been drawn to indicate how the phase shifts probably vary with energy.

B. Resonance Parameters

Because of the experimental analytical uncertainties in this work, it was decided simply to apply the one-level approximation to the appropriate phase shifts at resonances whether or not this approximation could otherwise be justified. This corresponds to using Breit-Wigner forms for the resonances. Therefore, uncertainties in the resulting values for the reduced width γ^2 might be as great as 30%. Consistent with this approximation, channels other than elastic scattering were ignored.

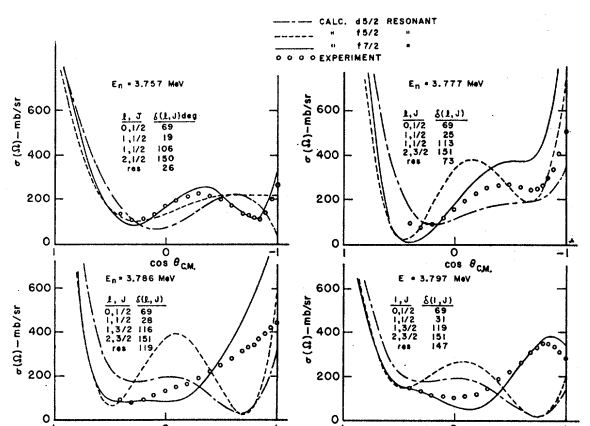

FIG. 13. Comparison of experimental and artifically generated angular distributions for $O^{16}(n,n)O^{16}$ in the vicinity of the resonance at $E_n=3.78$ MeV. The points represent the experimental results for a neutron energy spread of 18 keV and include correction for counter resolution. The various curves were calculated under the assumptions that the resonance is $d_{5/2}$, $f_{5/2}$, or $f_{7/2}$ and has a width of 22 keV.

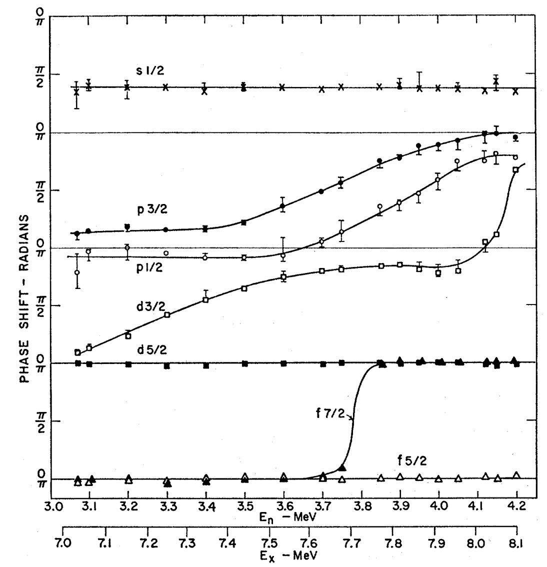

FIG. 14. The phase shifts for $O^{16}(n,n)O^{16}$ plotted as a function of neutron energy and excitation energy.

The phase shift $\delta(l,J)$ in the vicinity of an isolated (l,J) resonance corresponding to the unbound state λ, may be written as

$$\delta(l,J)=\beta_\lambda+\varphi(l,J),$$

where λ denotes all the quantum number of the state, $\varphi(l,J)$ is the nonresonant part of the phase shift and

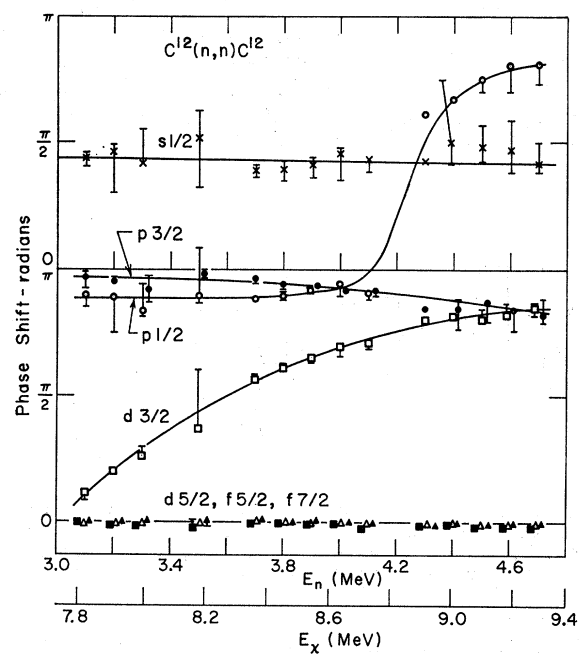

FIG. 15. The phase shifts for $C^{12}(n,n)C^{12}$ plotted as a function of neutron energy and excitation energy.

TABLE V. Level parameters for states of O^{17}.

E_n(MeV)	$E_R{}^a$(MeV)	E_λ(MeV)	J^π	$\Gamma_{c.m.}$(keV)	Γ_n/Γ	$\gamma_{\lambda n}{}^2$(MeV)	$\theta_{\lambda n}{}^2$	φ_λ(deg)
3.29 $\pm$0.02	7.24	7.02	$\frac{3}{2}+$	400$\pm$30	>0.99	0.25	0.15	−20
3.77 $\pm$0.02	7.69	7.67	$\frac{3}{2}-$	360$\pm$30	>0.99	0.12	0.07	+17
3.78 $\pm$0.01	7.70	7.60	$\frac{7}{2}-$	<23	>0.99	<0.05	<0.03	0
3.92 $\pm$0.02	7.83	7.82	$\frac{1}{2}-$	245$\pm$30	>0.95	0.07	0.04	−12
4.175$\pm$0.01	8.07	8.05	$\frac{3}{2}+$	75$\pm$20	>0.90	0.03	0.02	−23

[a] $E_R=(16/17)E_n+4.142$ MeV.

β_λ is the resonant part of the phase shift and is given by

$$\beta_\lambda=\tan^{-1}(\tfrac{1}{2}\Gamma_\lambda/E_R-E).$$

Γ_λ is the width of the level and E_R is the resonance energy, defined as the energy corresponding to $\beta_\lambda=\pi/2$.

Estimates of the various $\varphi(l,J)$ were made by inspection of the $\delta(l,J)$ versus E curves, guided by a reasonable extrapolation of the single-particle phase shifts of Kolesov *et al.*[28] The width Γ was taken as

$$E(\beta=135°)-E(\beta=45°)$$

or

$$2|E(\beta=90°\pm45°)-E(\beta=90°)|,$$

if the latter was more practical.

First-order expressions relating the experimental parameters to R-matrix parameters[29] are given by (c.m. system is implied).

$$\Gamma_\lambda=2P_l\gamma_\lambda{}^2,$$
$$\theta_\lambda=\gamma_\lambda{}^2/(\hbar^2/ma_c{}^2),$$
$$E_R=E_\lambda+\Delta_\lambda,$$
$$\Delta_\lambda=-S_l\gamma_\lambda{}^2,$$

P_l is the penetrability, $\gamma_\lambda{}^2$ the reduced width, $\theta_\lambda{}^2$ the dimensionless reduced width, a_c the channel radius, m the reduced mass, E_λ the characteristic energy, Δ_λ the level shift, and S_l the shift factor. $\theta_\lambda{}^2$ may be compared to $\theta_c{}^2$, the single-particle reduced width for a given channel. $\theta_c{}^2=\frac{3}{2}$ times the quantity usually referred to

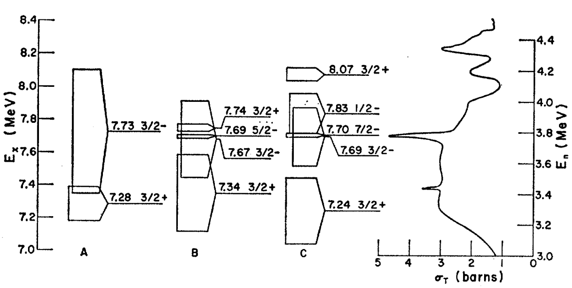

FIG. 16. A graphical presentation of level parameters assigned to states of O^{17}, according to (A) Baldinger, Huber, and Proctor (Ref. 3), (B) Fowler and Johnson (Ref. 9), and (C) this work. The total neutron cross section of oxygen is shown on the same energy scale.

[29] A. M. Lane and R. G. Thomas, Rev. Mod. Phys. 30, 257 (1958).

as the Wigner limit on the reduced width. A reasonable but rough estimate of the magnitude of $\theta_c{}^2$ is 0.5.[30]

VI. CONCLUSION

Application of the phase-shift analysis program to the $O^{16}(n,n)O^{16}$ differential cross sections, as described in Sec. V, was successful in assigning level parameters to five levels of O^{17} in the excitation energy range between 7.2 and 8.1 MeV. These are listed in Table V. Above an excitation energy of about 8.1 MeV either the levels were too narrow, or the level structure was too complex to be handled by the phase-shift analysis program. All the levels considered in this study are $T=\frac{1}{2}$ since the lowest $T=\frac{3}{2}$ level in O^{17} would probably correspond to the N^{17} ground state and have an energy of about 11.2 MeV.[31]

Figure 16 is a comparison of O^{17} level parameters found in this and in previous studies. The broad, overlapping $\frac{3}{2}+$, 7.24 MeV and $\frac{3}{2}-$, 7.69-MeV levels found in this work are in fair agreement with the results of Baldinger *et al.*,[3] and Fowler and Johnson.[9] The assignment of $\frac{7}{2}-$ to the 7.70-MeV level is in disagreement with the interpretation of Fowler and Johnson, who found that a combination of a $\frac{5}{2}-$ and a $\frac{3}{2}+$ resonance best suited their data in this energy region. It may be mentioned, however, that the differential cross-section results of this work and the work of Fowler and Johnson are in good agreement. Other assignments to this level have been $J=\frac{5}{2}$ by Fossan *et al.*,[22] and $J\geq\frac{5}{2}$ by Walton, Clement, and Boreli.[13] The basis of the $\frac{7}{2}-$ assignment from the present work was the comparison of the various computed angular distributions with those measured in the vicinity of the resonance, as typified by Fig. 13. Furthermore, the behavior of the coefficient B_5 in Fig. 11 near $E_n=3.78$ MeV is well explained by the interference between the $\frac{7}{2}-$ and $\frac{3}{2}+$ phase shifts. In order to account similarly for such behavior in B_5, a $\frac{5}{2}-$ resonance would have to be accompanied by a considerable negative amount of $J\geq\frac{5}{2}$, positive parity phase shift, which is not required at other energies.

The $\frac{1}{2}-$, $E_x=7.83$-MeV level reported here may perhaps be identified with the $J=\frac{1}{2}$, 110-keV wide level at 7.94 MeV observed in $C^{13}(\alpha,n)O^{16}$ work[13] and later

[30] F. C. Barker, Nucl. Phys. 28, 96 (1961).

[31] T. Lauritsen and F. Ajzenberg-Selove, in *American Institute of Physics Handbook* (McGraw-Hill Book Company, Inc., New York, 1963), 2nd ed., Chap. 8, p. 79.

TABLE VI. Level parameters for states of C^{13}.

E_n[a](MeV)	E_R[a](MeV)	E_λ(MeV)	J^π	$\Gamma_{c.m.}$(keV)	Γ_n/Γ	$\gamma_{\lambda n}$(MeV)	$\theta_{\lambda n}^2$	φ_λ(deg)
3.60±0.05	8.27	7.96	$\frac{3}{2}+$	1050±100	>0.99	0.68[b]	0.35[b]	0
4.25±0.02	8.87	8.86	$\frac{1}{2}-$	180±50	>0.99	0.06	0.03	−22

[a] E_n is the laboratory neutron energy at resonance; i.e., $\beta=90°$. $E_R=(12/13)E_n+4.947$ MeV.
[b] If the more exact expression for γ^2 is used, which takes into account the first-order energy dependence of the shift factor, these values are increased by about 30%. They represent about half the single-particle values.

assigned negative parity by means of the $C^{13}(\alpha,\alpha)C^{13}$ interaction.[32] It is possible that the true values for the width and energy of this level may be distorted in $C^{13}+\alpha$ studies because of the rapid increase of the Coulomb barrier penetrability with energy in the $C^{13}+\alpha$ channel. In any case our $\frac{3}{2}+$ assignment to the 8.07-MeV level agrees with the combined results of $C^{13}+\alpha$ work.[13,32,33]

Although the $O^{16}(n,n)O^{16}$ phase shifts could not be obtained in this work above $E_n\sim4.2$ MeV($E_x=8.1$ MeV), some comments may be made regarding the 4.3- to 4.5-MeV region, where total neutron cross-section work indicates the existence of one or more resonances of width ≥50 keV. Baldinger *et al.*[3] found a $\frac{1}{2}-$, $\Gamma_{c.m.}=250$-keV level at $E_n=4.40$ MeV. Fossan *et al.*[22] found a $J=\frac{3}{2}$, $\Gamma_{c.m.}=60$ keV, resonance at $E_n=4.32$ MeV from their total neutron cross-section work on O^{16}. Studies[13,33] of $C^{13}(\alpha,n)O^{16}$ indicated the presence of a $J=\frac{3}{2}$, $\Gamma_{c.m.}=60$ keV, resonance at an energy corresponding to E_n of about 4.30 MeV. Resonances were observed in the $C^{13}(\alpha,\alpha)C^{13}$ work of Barnes *et al.*,[32] at energies corresponding to lab neutron energies for $O^{16}+n$ of 4.32, 4.45, and 4.50 MeV and given spin-parity assignments of $\frac{3}{2}-$, probably $\frac{1}{2}+$, and $\frac{5}{2}-$, respectively. We note that the observed peaking of the coefficient B_3 near 4.36 MeV in Fig. 10 would seem to require either two overlapping $\frac{3}{2}$ resonances of opposite parity or a resonance of $J\geq\frac{5}{2}$ interfering with a non-negligible phase shift of opposite parity.

If the principle of charge symmetry holds, then there should be a correspondence between states of O^{17} and its mirror nuclues F^{17}. Level parameters of states of F^{17} have been obtained by Salisbury and Richards[34] from 2.6 to 7.4 MeV of excitation and by Dangle *et al.*[35] from 7.3 to 9.1 MeV. Reference 34 shows excellent correspondences between levels in O^{17} and F^{17} up to about 6.5 MeV. Table VII lists possible analog states in the energy region considered in the present work.

Only two levels in C^{13} were observed between 7.78 and 9.32 MeV excitation energy. They are listed in Table VI. The broad $\frac{3}{2}+$, 8.3-MeV level has previously been identified by Wills *et al.*,[19] and by Meier, Scherrer, and Trumpy.[20] Its dimensionless reduced width, θ^2 has a value of about one-half the single-particle value.[36] We have found the $J=\frac{1}{2}$, 8.85-MeV level, previously observed in total cross-section work,[22,37] to have negative parity. These states correspond to the $\frac{3}{2}+$, 8.1 MeV and $\frac{1}{2}-$ 8.90-MeV levels, respectively, in N^{13}, which have been investigated by Shute *et al.*[36] Theoretical studies by Kurath[38] and Barker[30] on positive parity states in C^{13} predict a state corresponding to the $\frac{3}{2}+$, 8.3-MeV level. Kurath and Lawson[39] have studied the negative parity states of mass 13 nuclei and predict a $\frac{1}{2}-$ level which, for a reasonable value of their parameter a/K of 5.3, can be identified with the above-mentioned $\frac{1}{2}-$ levels in C^{13} and N^{13}.

The $O^{16}(n,\alpha)C^{13}$ total cross section measured in this experiment is compared to the measurements of Walton, Clement, and Boreli[13] and Seitz and Huber[40] in Fig. 8. Agreement is reasonably good. At worst, the results of this work lie below those of Walton, Clement, and Boreli by about 30%, which is within the combined experimental errors. To about the same extent the present results are in agreement with the cross section[13] of the inverse reaction, $C^{13}(\alpha,n)O^{16}$, through the principle of detailed balance.

Theoretical calculations in O^{17} have so far been limited to identifying the single-particle states,[41] that is, $\frac{5}{2}+$, g.s.; $\frac{1}{2}+$, 0.871 MeV; $\frac{3}{2}+$, 5.07 MeV; the indication by Christy and Fowler[42] that the $\frac{1}{2}-$, 3.06-MeV state has the configuration $(1p)^{-3}(2s,1d)^4$, and the suggestion by Harvey[43] that the $\frac{1}{2}-$, 5.94-MeV level is the lowest level in a $K=\frac{1}{2}-$ band.

TABLE VII. Corresponding energy levels of O^{17} and F^{17}.

O^{17}			F^{17} [a]		
J^π	E_x[b] (MeV)	θ^2	J^π	E_x[b] (MeV)	θ^2
$\frac{3}{2}+$ [c]	7.24	0.15	$\frac{3}{2}+$	7.21	0.19
$\frac{3}{2}-$ [d]	7.69	0.07	$\frac{3}{2}-$	8.22	0.09
$\frac{7}{2}-$	7.70	<0.03	$\frac{7}{2}-$	7.55	0.013

[a] Values taken from Refs. 34 and 35. Here, θ^2 is the quantity $\gamma^2/(3\hbar^2/2\mu a)$ for elastic scattering multiplied by $\frac{3}{2}$.
[b] E_x has been taken to be equal to E_R as defined in the text.
[c] Correspondence made in Ref. 34.
[d] Correspondence made in Ref. 35.

[32] B. K. Barnes, R. L. Steele, T. A. Belote, and J. R. Risser, Bull. Am. Phys. Soc. **8**, 125 (1963).
[33] J. P. Schiffer, A. A. Kraus, Jr., and J. R. Risser, Phys. Rev. **105**, 1811 (1957).
[34] S. R. Salisbury and H. T. Richards, Phys. Rev. **126**, 2147 (1962).
[35] R. L. Dangle, L. D. Oppliger, and G. Hardie, Phys. Rev. **133**, B647 (1964).
[36] G. G. Shute, D. Robson, V. R. McKenna, and A. T. Berztiss, Nucl. Phys. **37**, 535 (1962).
[37] K. Tsukada and T. Fuse, J. Phys. Soc. Japan **15**, 1994 (1960).
[38] D. Kurath, Phys. Rev. **101**, 216 (1956).
[39] D. Kurath and R. D. Lawson, Nucl. Phys. **23**, 5 (1961).
[40] J. Seitz and P. Huber, Helv. Phys. Acta **28**, 227 (1955).
[41] A. M. Lane, Rev. Mod. Phys. **32**, 519 (1960).
[42] R. F. Christy and W. A. Fowler, Phys. Rev. **96**, 851 (1954).
[43] M. Harvey, Phys. Letters. **3**, 209 (1963).

In view of the present existence of a large body of spectroscopic information in the O^{17} and F^{17} systems extending from the ground state to excitation energies of about 8 MeV, there is a need at this point for more detailed theoretical study of the $A=17$, $T=\frac{1}{2}$ system. In particular, resonances of moderate reduced widths observed in the $O^{16}+n$ interaction would probably be associated with states of O^{17} having configurations that couple fairly strongly to the continuum. Comparison of theory with experiment then would shed light on both the form of the interaction and the configurations of the intermediate states involved.

PHYSICAL REVIEW VOLUME 143, NUMBER 3 MARCH 1966

Dependence of Proton Optical-Model Parameters upon Experimental Uncertainties*

J. K. DICKENS
Oak Ridge National Laboratory, Oak Ridge, Tennessee
(Received 22 September 1965)

The dependence of proton optical-model parameters upon experimental uncertainties has been studied for four types of errors. These were errors in over-all normalization, errors affecting the shape of the angular distribution, errors in incident energy, and errors in scattering angle. By varying the data, it is found that the optical-model parameters are affected differently by the four types of errors; this suggests that a single, over-all assigned error is inadequate for error analysis in optical-model studies. The minimum-χ^2 criterion is critically examined as a criterion for obtaining optimum optical-model parameters. The role of the experimental errors in the theoretical analysis is studied. Because the errors associated with the individual cross sections that form an angular distribution are not independent, we conclude that these data do not make up a collection of several independent random samples, but that, collectively, they resemble a single random sample. This conclusion is statistically important in the study of reaction mechanisms using results of optical-model analysis.

I. INTRODUCTION

RECENT systematic optical-model analysis of proton elastic scattering from elements heavier than Al showed that good fits to the experimental data could be obtained.[1] Excellent fits to experimental data for E_p between 9 and 22 MeV were obtained when most of the parameters of the model were allowed to vary; however, the resulting best-fit parameters exhibited considerable variation from one angular distribution to the next. When large fluctuations in the parameters as a function of mass number and energy are necessary to describe the scattering, the usefulness of an optical-model description is much reduced.

To make the optical-model description more useful in the proton analysis[1] an average set of geometrical parameters was obtained to determine whether the data could be reproduced with smoothly varying real and imaginary well depths. A distinctive feature of this analysis was that the data were very adequately reproduced by the predictions of this restricted model, and the variations in the well-depth parameters were substantially reduced.

The next goal has been to ascertain if there is a systematic variation of these parameters as a function of mass number which might yield information about the mechanisms involved in the reaction. An example is the suggestion of Lane[2] that the real optical potential should exhibit an isobaric spin dependence. For nucleon elastic scattering this dependence results in a nuclear-symmetry term in the optical potential of the form

$$\pm V_1(N-Z)/A\,, \qquad (1)$$

where the $+$ and $-$ signs refer to neutrons and protons, respectively. Several groups[1,3–9] have attempted to obtain a value for V_1 by studying proton elastic scattering; results from some of these studies are presented in Table I. Examination of Table I shows that all of the values are reasonably consistent with $V_1 \simeq 25$ MeV except that of Durisch and Gould.[6] The tin data they analyzed were reported with a precision of $\pm3\%$,[10] a

* Research sponsored by the U. S. Atomic Energy Commission under contract with Union Carbide Corporation.

[1] F. G. Perey, Phys. Rev. **131**, 745 (1963).

[2] A. M. Lane, Nucl. Phys. **35**, 676 (1962).

[3] J. Benveniste, A. C. Mitchell, and C. B. Fulmer, Phys. Rev. **129**, 2173 (1963).

[4] J. Benveniste, A. C. Mitchell, B. Buck, and C. B. Fulmer, Phys. Rev. **133**, B323 (1964).

[5] J. B. Ball, C. B. Fulmer, and R. H. Bassel, Phys. Rev. **135**, B706 (1964).

[6] J. E. Durisch and P. Gould, Phys. Rev. **137**, B906 (1965).

[7] R. C. Barrett, A. D. Hill, and P. E. Hodgson, Nucl. Phys. **62**, 133 (1965).

[8] P. C. Sood, Nucl. Phys. **37**, 624 (1962).

[9] G. R. Satchler, R. M. Drisko, and R. H. Bassel, Phys. Rev. **136**, B637 (1964).

[10] J. E. Durisch, R. R. Johnson, and N. M. Hintz, Phys. Rev. **137**, B904 (1965).